Nanoassembly of Polydisperse Photonic Crystals Based on Binary and Ternary Polymer Opal Alloys

Zhao, Qibin; Finlayson, Christopher; Schafer, Christian G.; Spahn, Peter; Gallei, Markus; Herrmann, Lars; Petukhov, Andrei; Baumberg, Jeremy J.

Published in:
Advanced Optical Materials

DOI:
10.1002/adom.201600328

Publication date:
2016

Citation for published version (APA):
Zhao, Q., Finlayson, C., Schafer, C. G., Spahn, P., Gallei, M., Herrmann, L., Petukhov, A., & Baumberg, J. J. (2016). Nanoassembly of Polydisperse Photonic Crystals Based on Binary and Ternary Polymer Opal Alloys. *Advanced Optical Materials* , *4*(10), 1494-1500. https://doi.org/10.1002/adom.201600328

ADVANCED OPTICAL MATERIALS

Supporting Information

for *Adv. Optical Mater.,* DOI: 10.1002/adom.201600328

Nanoassembly of Polydisperse Photonic Crystals Based on Binary and Ternary Polymer Opal Alloys

*Qibin Zhao, Chris E. Finlayson, Christian G. Schaefer, Peter Spahn, Markus Gallei, Lars Herrmann, Andrei V. Petukhov, and Jeremy J. Baumberg**

Supporting Information

for *Adv. Opt. Mater.*, DOI: 10.1002/adom.201600328

Nanoassembly of Polydisperse Photonic Crystals based on Binary and Ternary Polymer Opal Alloys

*Qibin Zhao, Chris E. Finlayson, Christian Schafer, Peter Spahn, Markus Gallei, Lars Herrmann, Andrei Petukhov, and Jeremy J. Baumberg**

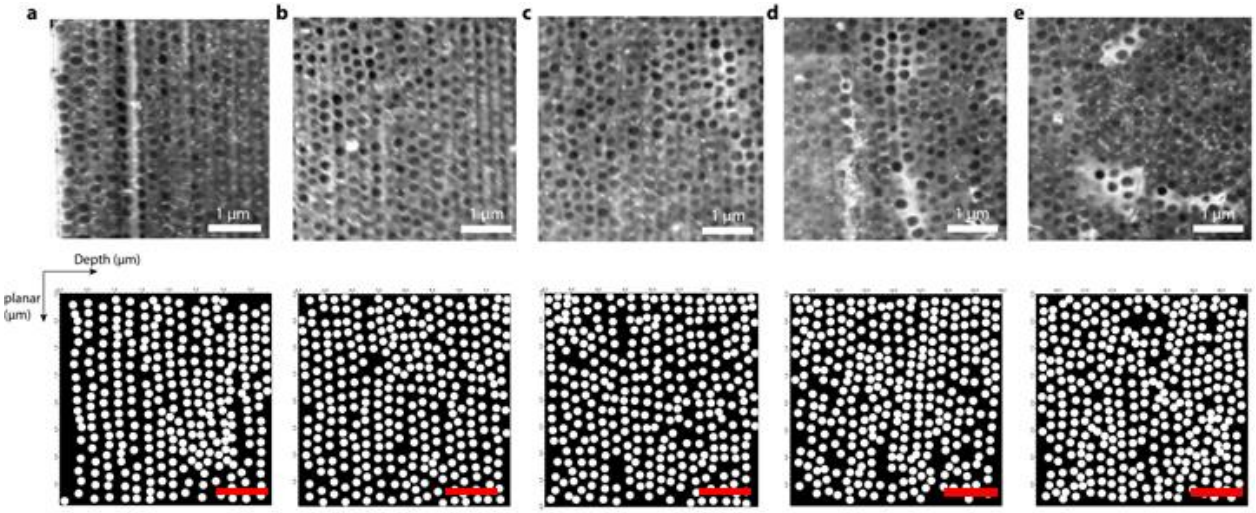

Figure S1. SEM images of the cross sections of G:R = 1:1 PO alloy sample with 40 passes of BIOS, cross sections trimmed by FIB. (a – e) Cross-sections in depth direction from 0 µm to 20 µm, each image being 4µm deep. Binary images below each SEM image show positions of spheres after fitting, sphere diameters set to 182 nm. The images are at the same scale as the SEM images, with the scale bar representing 1 µm.

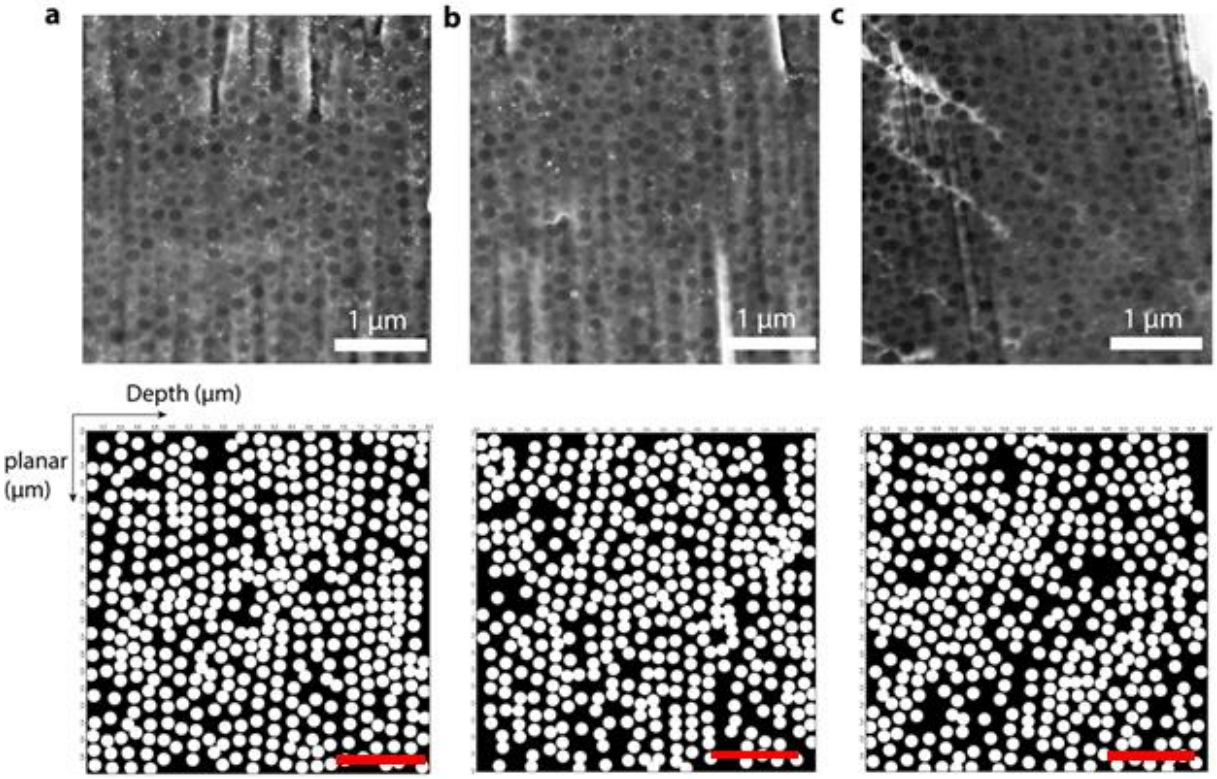

Figure S2. SEM images of cross sections of B:G:R = 3:2:1 PO alloy sample with 40 passes of BIOS, cross sections trimmed by FIB. (a – c) Cross-section in the depth direction from 4 µm to 16 µm, each image being 4µm deep. Binary images below each SEM image show positions of spheres after fitting, sphere diameters set to 182 nm. The images are at the same scale as the SEM images, with the scale bar representing 1 µm.

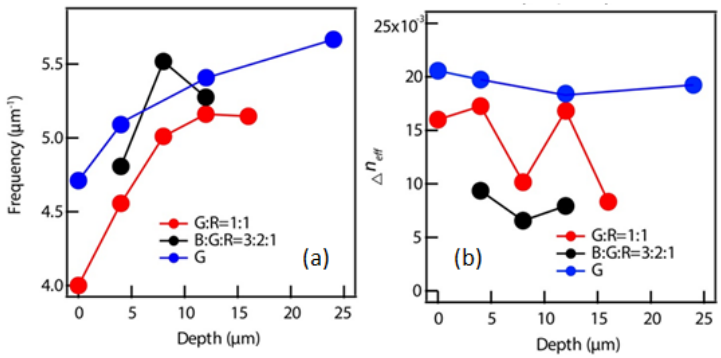

Figure S3. (a) Extracted spatial frequency in depth direction for single, binary and ternary POs. (b) Extracted effective refractive index contrast Δn_{eff} along depth direction of single, binary and ternary POs.

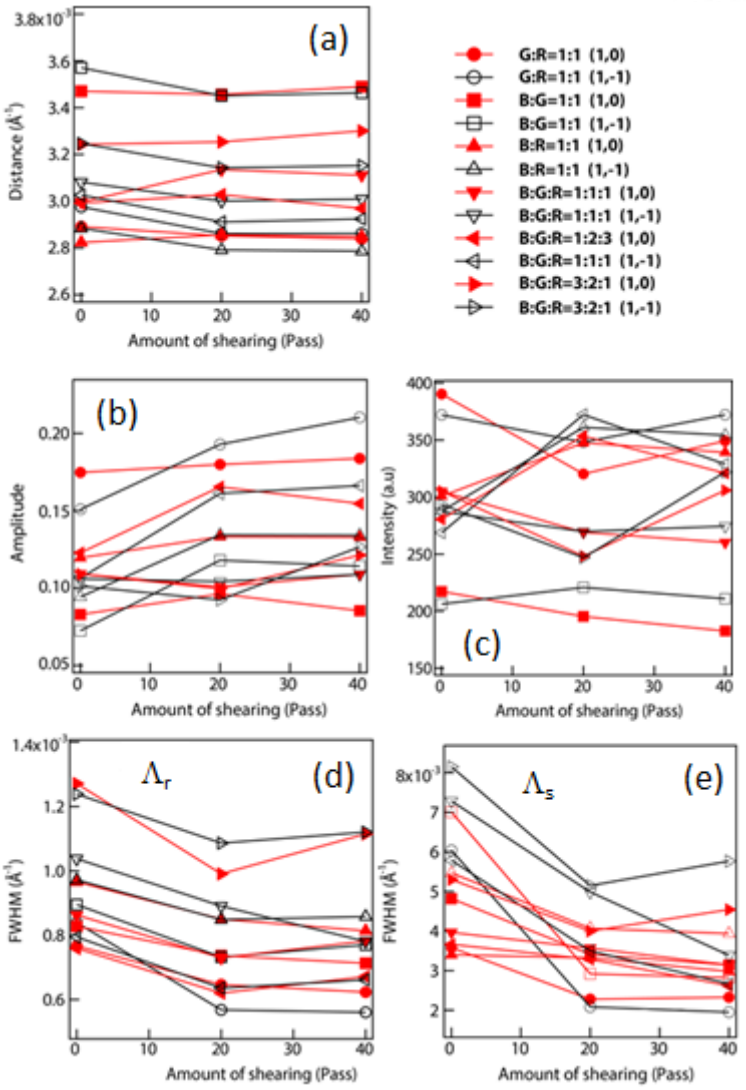

Figure S4. Analysis of SAXS results for binary and ternary PO alloys before and after BIOS at normal incidence. (a) Change of distance from centres of spots (10) and $(1\bar{1})$ to origin in reciprocal space with increasing BIOS shearing. (b) Change of spot amplitudes with increasing BIOS passes. (c) Change of spot intensities (areas) with increasing BIOS passes. (d) Change of FWHM in radial direction of spots Λ_r (short axis of spots) with increasing BIOS shearing. (e) Change of FWHM in long axis (azimuthal direction) of spots Λ_s with increasing BIOS passes.

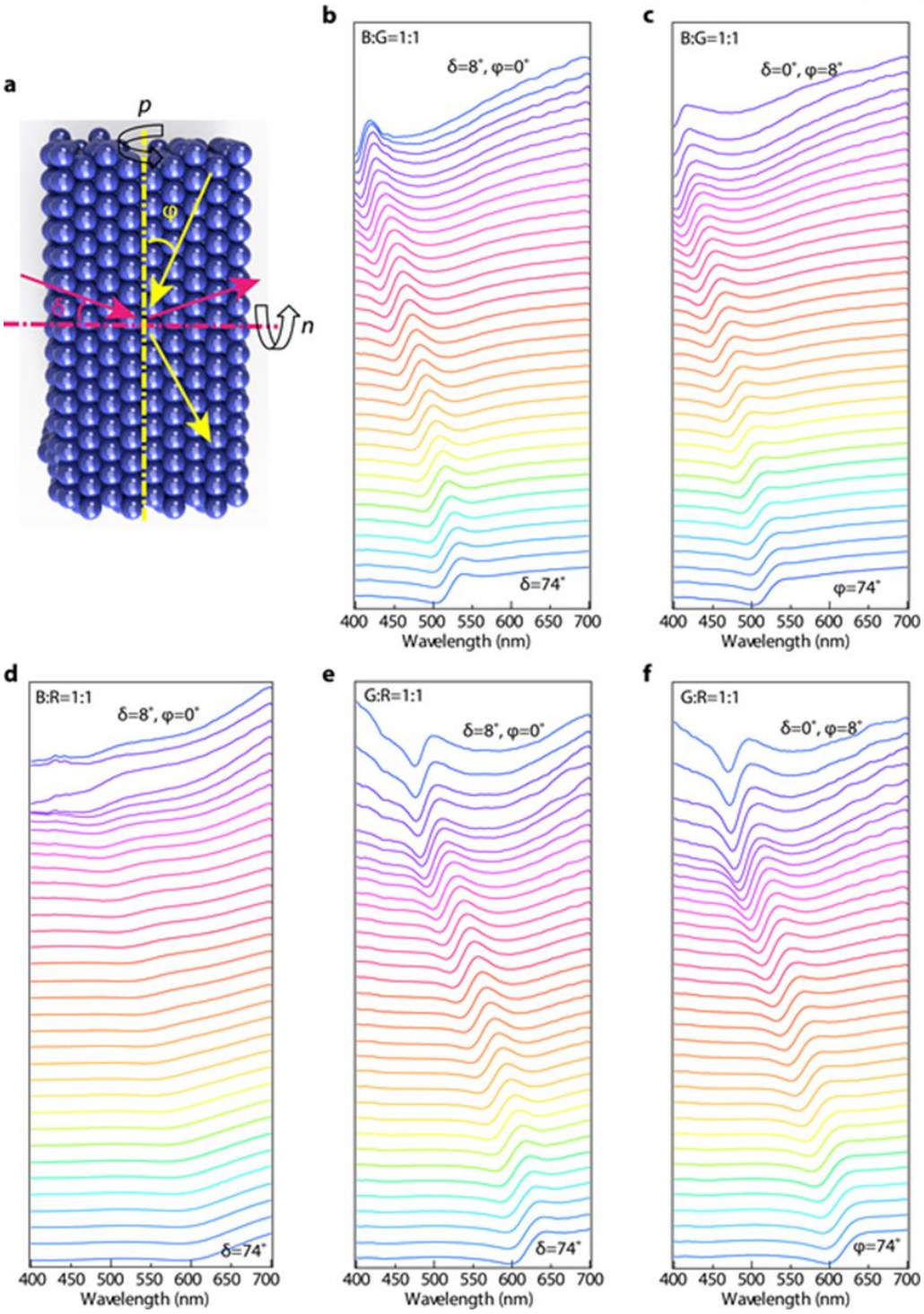

Figure S5. Angle-dependent specular reflection of different binary PO alloys measured with goniometer. (a) Schematic view of measurement geometry, with δ and ϕ representing the angle between the incident light and the surface of the sample. When incident light goes along the *p* axis with an angle of 8 degrees, δ=8 and ϕ varies from 0 to 74°. When incident light goes along the *n* axis with an angle of 8 degrees, δ varies from 0 to 74°, and ϕ=8. (b-f) Measured spectra of different samples at different orientations, as indicated.